© 2017. Published by The Company of Biologists Ltd | Journal of Experimental Biology (2017) 220, 4095-4100 doi:10.1242/jeb.166629

Giving invertebrates an eye exam: an ophthalmoscope that utilizes the autofluorescence of photoreceptors

Annette Stowasser, Madeline Owens and Elke K. Buschbeck*

ABSTRACT

One of the most important functional features of eyes is focusing light, as both nearsightedness and farsightedness have major functional implications. Accordingly, refractive errors are frequently assessed in vertebrates, but not in the very small invertebrate eyes. We describe a micro-ophthalmoscope that takes advantage of autofluorescent properties of invertebrate photoreceptors and test the device on the relatively well-understood eyes of jumping spiders and flies. In each case, our measurements confirmed previous findings with a greater degree of accuracy. For example, we could precisely resolve the layering of the anterior median eyes and could map out the extensive retina of the anterior lateral eyes of the spider. Measurements also confirmed that fly ommatidia are focused into infinity, but showed that their focal plane is situated slightly below the receptor surface. In contrast to other approaches, this device does not rely on reflective tapeta and allows for precise optical assessment of diverse invertebrate eyes.

KEY WORDS: Optics, Spiders, Flies, Retina, Invertebrate vision, Refractive error

INTRODUCTION

One of the most important features of any eye is its ability to correctly focus light onto the retina, a process that requires tight coordination between the optical properties of the lens and the spacing between the lens and retina. Accordingly, many studies exist in vertebrates that investigate how correct focusing is established and maintained (Hung et al., 1995; Kroger and Wagner, 1996; McFadden et al., 2004; Schaeffel et al., 1988; Sivak, 2008). However, few studies have explored how invertebrate eyes are focused, with the most notable studies having been performed on the image-forming eyes of spiders (Land, 1969b), larval stemmata (Mizutani and Toh, 1995; Stowasser and Buschbeck, 2014), insect ocelli (Berry et al., 2007; Taylor et al., 2016) and the ommatidia of fly eyes (Franceschini and Kirschfeld, 1971; Kirschfeld and Franceschini, 1968). However, the majority of refractive state assessments in these animals used indirect methods that are difficult to conduct and suffer from some inherent inaccuracies. In addition, studies on how correct focusing is established are almost entirely absent in invertebrates, though it recently has been shown that in cephalopods (Turnbull et al., 2015), like in vertebrates (Flitcroft, 2013; McBrien and Barnes, 1984; Wallman and Winawer, 2004), this process requires visual input. Considering the many molecular (Cook and Desplan, 2001; Cook et al., 2011; Freund et al., 1996), functional (Land and Nilsson, 2012) and neurological (Sanes and Zipursky, 2010) similarities between vertebrate and invertebrate eyes, there is a strong need for such studies in invertebrates, but these require tools that rapidly and accurately assess refractive properties in very small eyes. Such tools are currently unavailable, as conventional methods do not work on eyes at the scale found in most invertebrates.

Nearly 50 years ago, Mike Land developed an ophthalmoscope (Land, 1969a,b) to directly measure refractive properties of jumping spider eyes. Although this tool was limited to eyes with tapeta or other reflective structures that return incoming light, it has greatly enhanced our understanding of invertebrate optics. In addition to the work on jumping spiders, it has been used to assess optical parameters of the spider *Cupiennius salei* (Land and Barth, 1992) and to visualize the retina of other spiders (Nilsson et al., 1992). It also was used to measure the resolving power of butterflies (Land, 1984, 1990) and hummingbird hawkmoths (Warrant et al., 1999), to investigate the eye shine of butterflies (Stavenga, 2002) and the pupil reflex mechanism of insect apposition eyes (Nilsson et al., 1992; Nordstrom and Warrant, 2000). However, perhaps because of its restriction to reflective eyes, this method seems to have been largely forgotten since then. To develop a more widely accessible tool, we re-created and modified the 'Land-ophthalmoscope' so that it can be applied to a wider range of invertebrate eyes. Relying on the autofluorescence of photoreceptors (Franceschini, 1977; Franceschini et al., 1981; Kruizinga and Stavenga, 1990; Stark et al., 1977; Stavenga, 1983) instead of tapetal reflections, our micro-ophthalmoscope is suitable to measure eyes ranging from the relatively large eyes of jumping spiders to the very small individual ommatidia of compound eyes of flies. The autofluorescence of photoreceptors has previously been used to investigate opsin properties (Franceschini, 1983) and as an *in vivo* screening tool for *Drosophila* mutants (Pichaud and Desplan, 2001). However, to the best of our knowledge, this is the first time it has been utilized to measure the refractive state of invertebrate eyes.

To demonstrate the versatility and power of our micro-ophthalmoscope, we show that this tool allows us to independently image and measure the two deepest layers of the anterior medial (AM) eye of *Phidippus audax* jumping spiders. In fact, our tool is so sensitive that it can even resolve the relatively minor refractive differences across the medial–lateral extent of the first layer, which is organized as a 'staircase' (Land, 1969b) so that photoreceptors are staggered between their medial and lateral extent. In addition, our methods allowed us to generate complete high-resolution retinal images of these spiders' anterior lateral (AL) eyes. Rhabdomere tips of flies also have been successfully imaged in the less-reflective compound eyes (Franceschini, 1975). To demonstrate that our imaging method extends to compound eyes, we evaluated the refractive state of individual ommatidia of flesh flies. Our results demonstrate that our micro-ophthalmoscope has great

Department of Biological Sciences, University of Cincinnati, Cincinnati, OH 45221, USA.

*Author for correspondence (elke.buschbeck@uc.edu)

E.K.B., 0000-0001-8563-0826

Received 14 July 2017; Accepted 12 September 2017

Journal of Experimental Biology (2017) 220, 4095-4100 doi:10.1242/jeb.166629

potential to serve as a valuable tool to visualize the retina, and to investigate the refractive state of live invertebrates with different eye types, even in the absence of a reflective structure. Given the large diversity of invertebrate eye types, and the availability of sophisticated molecular tools in *Drosophila*, we anticipate that this tool will allow researchers to address a large body of open questions relating to invertebrate eye development and function, at both the molecular and the organismal level.

MATERIALS AND METHODS

Ophthalmoscope design

The micro-ophthalmoscope is composed of two achromatic lenses (top lens: f=150 mm, AC254-150-A; accessory lens: f=200 mm, AC254-200-A; both Thorlabs, Newton, NJ, USA), an objective (4× UplanFL, 10× UPlanFl in the case of the jumping spider, 40× UPlanFl in the case of the flesh fly and 50× UMPlanFl in the case of *Drosophila melanogaster*; Olympus, Central Valley, PA, USA), and a light-sensitive camera (ORCA-Flash 4.0 V2 Digital CMOS, C11440-22CU, Hamamatsu, Hamamatsu City, Japan) with imaging software (HCImageLive 4.3.1.30, Hamamatsu). The accessory lens is mounted on an optical linear scale with digital readout (EL10 DRO and GS212 scale, Electronica Mechatronic Systems Pvt Ltd, Pune, Maharashtra, India) the display of which is mirrored into the video frame. Illumination consists of a mercury light illuminator for fluorescence imaging (ULH100HG and BX-RFA, Olympus) equipped with an Olympus Texas Red filter cube (Olympus, U-N31004) and a DAPI filter cube (Olympus, U-N31000), each containing a dichroic mirror. Although we did not specifically optimize these filter cubes for our organisms, it has been described for a variety of invertebrate photoreceptors that their metarhodopsin leads to red emission when excited with blue or green light (Cronin and Goldsmith, 1981; Franceschini et al., 1981; Juse et al., 1989; Stavenga, 1983).

The illumination unit also contains an adjustable aperture and field stop (modified to close the iris further) and neutral density filters (Fig. 1A,B). A motorized micromanipulator (DC3K with MS 314, Märzhäuser, Wetzlar, Germany) allows for the precise positioning of the animals.

The microscope portion of the ophthalmoscope (Fig. 1A) is set up so that an object placed in the focal plane of the objective is in focus of the camera (initially the lens of an animal eye). The accessory lens is then added (Fig. 1B) which allows imaging of the retina. For each objective, the accessory lens has a zero reference position, which yields a focused image of an object at infinity, and thus it is the accessory lens position that yields a focused image of the retina if an eye is focused for infinity (i.e. emmetropic). If the accessory lens needs to be shifted towards the objective to visualize the retina, the eye is myopic, and if it has to be shifted away from the objective, it is hyperopic. To perform quantitative assessment of the refractive error, the correlation between accessory lens shift (the shift from the zero reference position) and in-focus object distance needs to be established for each objective (Fig. 1C). Resulting values are used to fit the function $f(x)=f^2/x$ where f is the focal length of the objective, which also describes the relationship in the myopic domain. This correlation in conjunction with an independent focal length measurement of the eye's lens then allows calculation of the refractive state of the eye (see below). Fig. 1D illustrates how the 10× and 40× objectives lead to differently sized sharp images of an object (the sailboat image) placed at effective infinity (~1.5 m away), with the accessory lens at its respective zero positions.

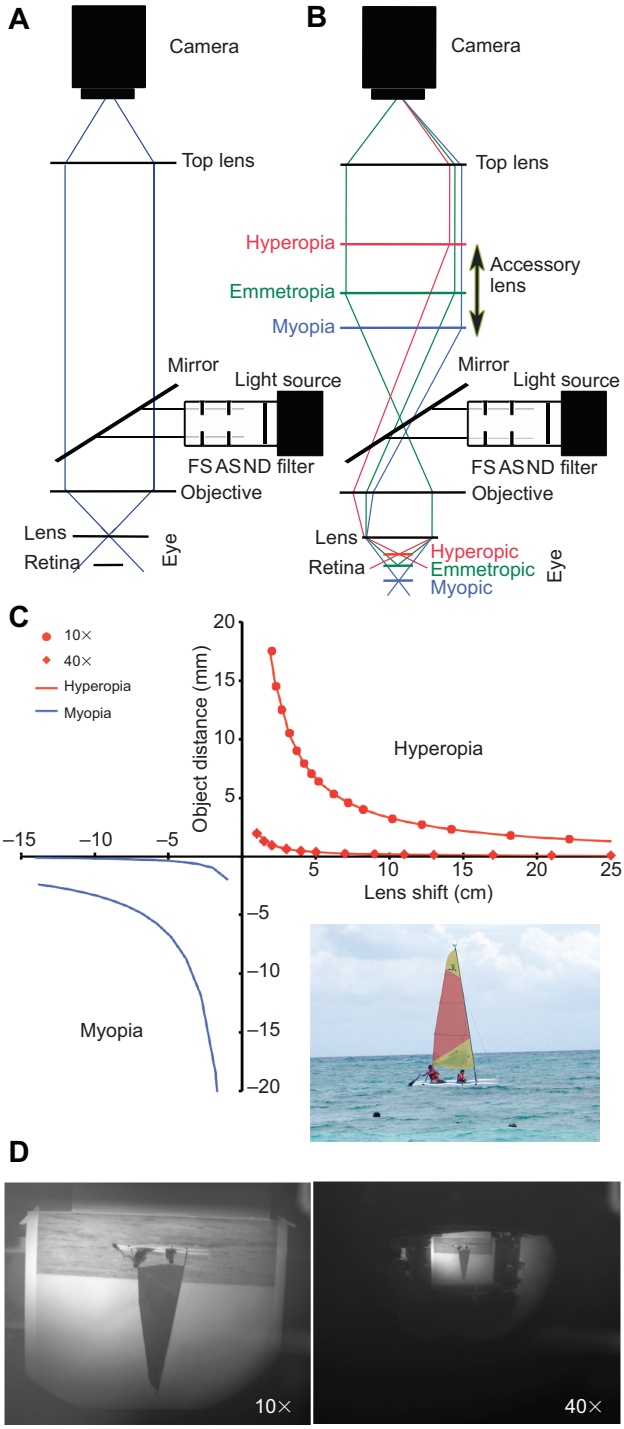

Fig. 1. Specifications of the ophthalmoscope. The ophthalmoscope consists of a camera, two lenses (top lens and accessory lens), a changeable objective and an epifluorescent light source that includes a dichroic mirror, and adjustable field (FS) and aperture (AS) stops as well as removable neutral density (ND) filters. (A) Without the accessory lens, the animal's lens is in focus. (B) With the accessory lens, the retina is in focus, with the refractive state of the eye determining the appropriate accessory lens position. (C) To determine how accessory lens position relates to in-focus object distance, objectives were calibrated by placing real objects at different distances and noting corresponding accessory lens positions. Symbols illustrate measured data points and solid lines represent best fits. (D) To illustrate the image quality of the ophthalmoscope, a calibration image (inset in C) was placed at effective infinity and mirrored into the 10× (left image) and 40× (right image) objectives while the accessory lens was in its zero position.

Journal of Experimental Biology (2017) 220, 4095-4100 doi:10.1242/jeb.166629

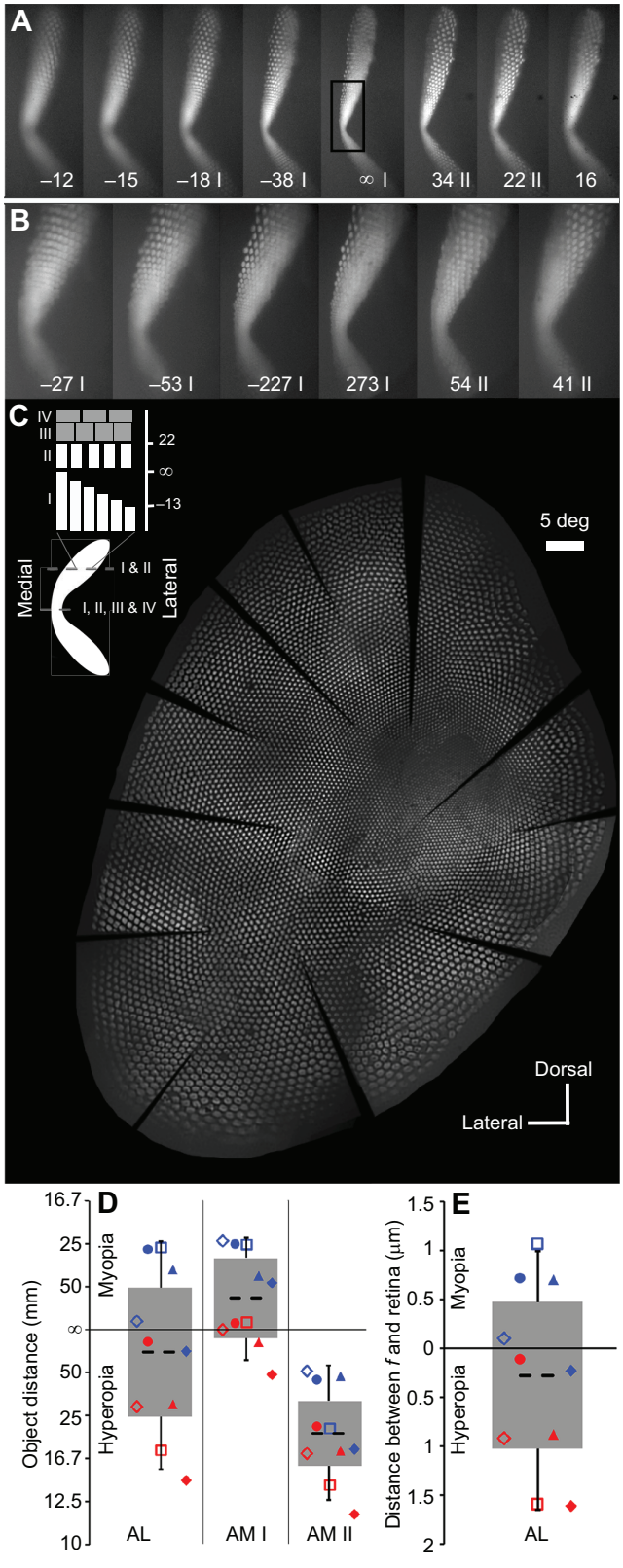

Fig. 2. Ophthalmoscope measurements of *Phiddipus audex*. (A) Example image series of the retina of a right anterior medial (AM) eye, clearly showing two layers (indicated as I or II). The numbers are corresponding object distances (in mm) that are in focus for those photoreceptors. Negative numbers are distances in front of the eye (indicating myopia) and positive numbers are object distances behind the eye (indicating hyperopia). (B) High magnification image series of the center of the boomerang of the eye shown in A. (C) An entire retina of an anterior lateral (AL) eye assembled from partial images that were taken after systematically adjusting the eye's angle. The scale bar is a visual field of 5 deg. The inset illustrates the tiered organization (Land, 1969b) of the retina of the AM eye with its four layers (I–IV). The numbers indicate the object distance (in mm) for which the surface of the corresponding photoreceptor array is in focus. (D) Ophthalmoscope measurements showing the object distances for which the retina of the AL eye and layers I and II of the AM eye are focused. The bars show the depth of focus with standard deviation. Each symbol shows the limits (blue towards myopia and red towards hyperopia) of the depth of focus for an individual (N=5). (E) The same data as in D for the AL eye, but expressed as the distance between the surface of the retina and the focal plane of the lens of the eye. No such values were provided for AM eyes, because they have a negative lens that further alters the position of the focal plane relative to the photoreceptors.

Ophthalmoscope measurements

To test the ophthalmoscope, we purchased juvenile jumping spiders, *Phiddipus audex* (Hentz 1845), from Phids.net (West Palm Beach, FL, USA) and flesh fly, *Sarcophaga bullata* (Parker 1916), pupae from Carolina Biological Supply Company (Burlington, NC, USA). We imaged each spider around maturation (N=5, cephalothorax length was between 2.7 and 4.2 mm) and each flesh fly post-eclosure (N=7). To demonstrate that the same technique also can be applied to *D. melanogaster*, we also imaged selected ommatidia of that species. For each measurement, the animal's lens was first brought into focus without the accessory lens, then the accessory lens was inserted and an image series of the retina was taken while shifting the accessory lens in both directions beyond the range of focus.

For each spider, we took image series of the retina of: (a) the AM eyes with the 10× objective (which was used to assess the refractive state) and with the 4× objective (for high magnification images of the retina) while the animal was anesthetized with CO_2 to prevent its retina from moving, and (b) the AL eyes with the 10× objective. To construct retinal maps of entire AL eyes (N=3), we took a series of images (at least 40 images per map) with the 10× objective while tilting and rotating the spider. Later, these images were assembled in Photoshop (Adobe, San Jose, CA, USA).

Imaging flies is somewhat tricky, because if more than one ommatidium is illuminated then the position of the deep pseudopupil is measured rather than the refractive properties of the ommatidia. To demonstrate this, we took image series (with the 40× objective) of the retina of *S. bullata* in the frontal region of their compound eyes while illuminating: (a) a single ommatidium and (b) multiple ommatidia. To recover autofluorescence, the eye was intermittently illuminated with UV light from an Olympus filter cube typically used for DAPI imaging. To demonstrate that such measurements also are possible in the very small *D. melanogaster*, we took images of their retina with the 50× objective.

To find the range of accessory lens positions that yielded focused images of the retina, each image series was blindly evaluated for best focus by two to three people. Corresponding object distances were calculated from the established correlation between accessory lens shift and object distance. These object distances, in conjunction with independent focal length assessment (see below), allowed us to determine the eye's refractive state quantitatively in terms of the distance between the surface of the photoreceptors and the focal plane of the eye's lens. This relationship is expressed as $\Delta f' = (f')^2/(n'o - f')$, where $\Delta f'$ is the distance between the surface of the photoreceptors and the focal plane of the eye, f' is the focal length of the animals' lens inside the eye (measured from the principal plane), n' is the refractive index behind the lens (assumed to equal that of

Journal of Experimental Biology (2017) 220, 4095-4100 doi:10.1242/jeb.166629

water; Land, 1969b; Williams and McIntyre, 1980) and o is the object distance (after Land, 1969b). Note that the focal length (f') in the denominator can be omitted if the object distance is much larger than the focal length, which is generally true unless the eye is very myopic or hyperopic. This equation was derived from the equation $n'/f'=n/o+n'/i$, where n is the refractive index of the medium in front of the lens (in our case air), n' is the refractive index behind the lens (in our case assumed to equal that of water), f' is the focal length behind the lens, o is the object distance and i is the image distance.

The focal length of the animal's lens was calculated from the image magnification (Land, 1969b; Land and Nilsson, 2012) following 'hanging-drop' procedures previously described (Homann, 1924; Stowasser et al., 2010). In brief, the isolated lenses were mounted with wax on top of Ringer solution (O'shea and Adams, 1981). To determine the image magnification, we used a compound scope for which we removed the condenser and took images through the animal's lenses (using a 10× objective for spiders, and a 20× objective for flies) of an object (USAF 1951 negative test target from Edmund Optics, Barrington, NJ, USA) that was placed at a distance from the animal's lens of 12.2 cm for spiders and 4.3 cm for flies. From the image magnification of the best-focused image, we then calculated the focal length behind the animal's lens (f'). For spiders, one of the AM and AL eyes was measured with both green and red light to evaluate chromatic aberration. For each flesh fly, we established the focal length of five randomly chosen ommatidia of the frontal region of one eye and used the other side of the head for histology.

RESULTS AND DISCUSSION

To demonstrate the applicability of the micro-ophthalmoscope, we focused our analysis on relatively well-understood optical systems to show that this method can replicate and even expand upon existing knowledge on their optics. The eyes we tested varied greatly in size and in the focal length of their lenses.

First, we investigated jumping spiders, the AM eyes of which are known to have multiple layers (Land, 1969b). We could independently image their layers I and II and even resolve the staircase organization of layer I (Fig. 2A,B), a schematic drawing of which is shown in Fig. 2C, inset. The staircase is discernible in that, in layer I, the lateral portion of the boomerang comes into focus before the medial portion as the accessory lens is adjusted. A higher magnification image illustrates how individual photoreceptors are well resolved in the periphery of the boomerang (Fig. 2B). We also imaged the retina of the AL eye and could generate entire retinal maps (Fig. 2C). In conjunction with focal length measurements of the lenses of AM and AL eyes, we quantified the refractive state of these eyes. In agreement with what has already been demonstrated for jumping spiders *Plexippus* (Blest et al., 1981), the difference between the focal length measured with red light (mean±s.d., AM

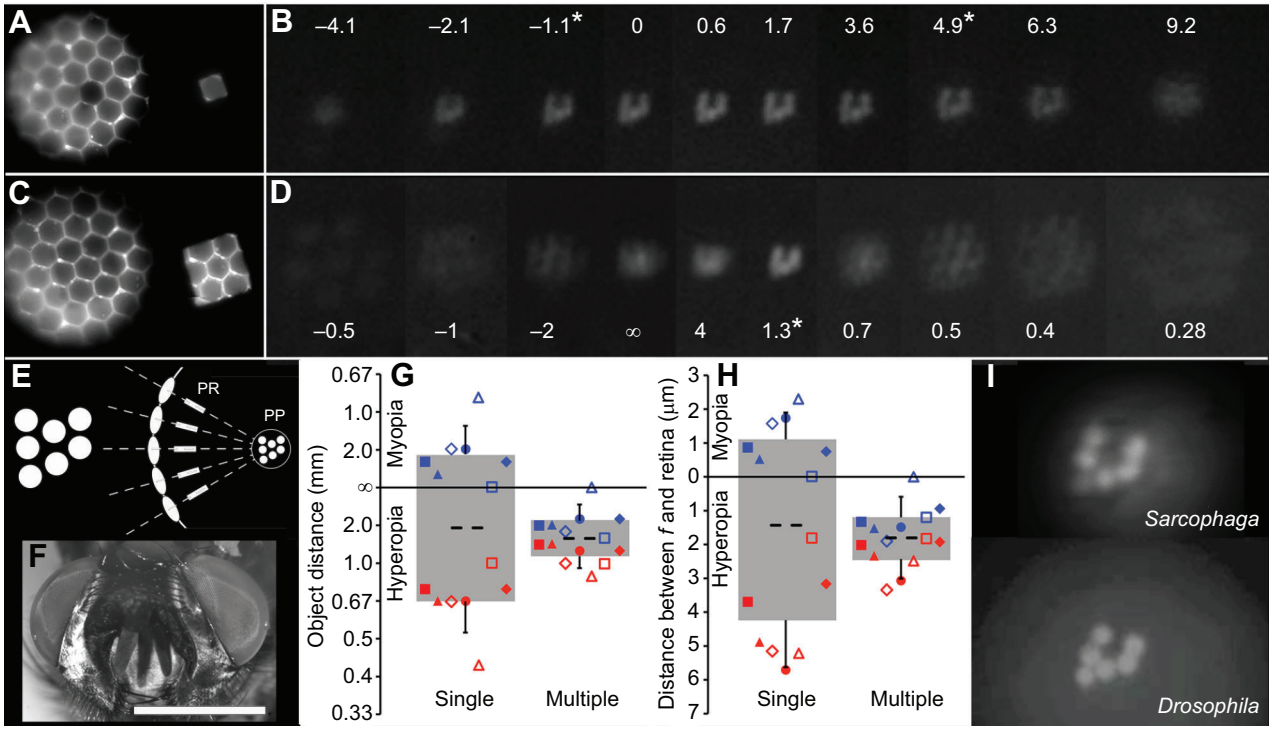

Fig. 3. Ophthalmoscope measurements of flies. (A) Post-measurement, the surface of a *Sarcophaga bullata* compound eye shows bleaching of a single ommatidium (left) that was selectively illuminated (right). (B) Resulting image series with the corresponding distance (in µm) between the focal plane of the lens of the ommatidium and the image plane at the level of the retina. (C) As in A, except that seven ommatidia were illuminated. (D) The image series that resulted from the illumination illustrated in C shows the narrowly focused pseudopupil (images were taken at the same accessory lens positions as for B). The numbers show corresponding object distances in mm. (E) Schematic diagram of the organization of the photoreceptors in each ommatidium (left). If multiple ommatidia are illuminated, the deep pseudopupil (PP) is imaged (right), as the images of multiple photoreceptor (PR) sets overlap in the center of the curvature of the compound eye. (F) External image of a *S. bullata* head; scale bar is 2 mm. (G) The bars show the average range of focus distances with standard deviation for the *S. bullata* dataset. The symbols illustrate the myopic (blue) and hyperopic (red) limits of the depth of focus for each individual (N=7). (H) When the lens's focal length has been established, then the distance between the surface of the retina and the position of an average lens's focal plane can be calculated. (I) Larger magnification of ophthalmoscope images showing the photoreceptors of both a single *S. bullata* and a single *Drosophila melanogaster* ommatidium. Asterisks in B and D mark the best-focused image of the series.

Journal of Experimental Biology

394.3±26.0 µm, AL 180.5±14.2 µm) and green light (AM 393±29.8 µm, AL 179.2±12.7 µm) was negligible (N=5) and hence we proceeded with optical calculations without correcting for chromatic aberration. For other lenses, calculations may have to be corrected based on the color-specific focal length measurements as established above, as photoreceptor autofluorescence typically produces red emission. Note that the optical components of the ophthalmoscope itself are very well corrected for chromatic aberration, as we could find no noticeable focus difference with different light illuminations. Consistent with previous findings (Land, 1969b), our measurements suggest that layer II of AM eyes is hyperopic, and layer I of the spider's AM eyes is situated around emmetropia. Specifically, we found that it was the medial portion of the staircase of layer I that was positioned around emmetropia (Fig. 2D), and that, in the same set of spiders, the range of focus of AM eyes was quite narrow when compared with that of their AL eyes (Fig. 2D). Our analysis further suggests that the lateral portion of the staircase is distinct from that of the medial portion, and provides sharp images into the near-field and striking range of the animal. It thus appears that the *P. audax* AM is well set up to obtain object distance-dependent photoreceptor activation within the staircase, which could be an important distance vision mechanism. Note that in *Hasarius adansoni*, image defocus is already thought to be important in that regard (Nagata et al., 2012). The central region of the retina of AL eyes was essentially emmetropic (Fig. 2E), with a comparatively wide range of depth of focus. Taken together, in regards to the spiders, we could easily resolve the refractive state of distinct retinal layers, and could even discern how portions of layer I are differentially focused.

For flies (Fig. 3F), visualization of the retina of both individual ommatidia (Fig. 3A,B,I) and multiple ommatidia (Fig. 3C,D) resulted in a clear image of the photoreceptor trapezoid. In the latter case, images of multiple retinas overlapped and hence we imaged the deep pseudopupil located in the center of the curvature of the eye (Fig. 3E), rather than individual receptors. The average focal length of *S. bullata* ommatidia was 50±7.4 µm (mean±s.d., N=7). The single ommatidium was essentially emmetropic and had a wide range of focus (Fig. 3G,H). This confirms that fly ommatidia are focused at infinity (Kirschfeld and Franceschini, 1968). Beyond what had been known, we found that (as might be expected for optimal sampling) the center of focus in *S. bullata* lies a few micrometers below the distal tips of the photoreceptors (Fig. 3H), but its depth of focus is large enough to allow ommatidia to see into infinity (Fig. 3B,G). In contrast, when we imaged the deep pseudopupil, the perceived depth of focus was extremely tight (Fig. 3D,G,H). This, for the first time, confirms through direct measurements that the pseudopupil lies near the center of curvature of the eye, as had already been inferred by indirect methods and theoretical considerations (Franceschini, 1972).

Our results show low variation and the method is a direct *in vivo* assessment that allows animals to survive seemingly unharmed. In addition to measuring the refractive state, our methods allowed us to evaluate the depth of focus, an important optical property that has received little attention despite its potentially profound functional implications. Our method takes all optical components into account, and thus promises to be more reliable than any of the indirect methods, opening the possibility to investigate many heretofore-inaccessible questions. These include, for example, molecular-genetic manipulations aimed at elucidating mechanisms that are involved in allowing eyes to establish correct focusing, or whether and how focusing is related to the circadian rhythm (Eckert, 1968; Horridge and Giddings, 1971; Menzi, 1987). As has been previously demonstrated (Land, 1984, 1969b), the ophthalmoscope also can be used to measure the receptor resolution by projecting an object of known angular extent (such as the aperture stop of the illuminator) onto the retina. As the method is not invasive, it can even be applied to longitudinal studies. Hopefully, the versatility of this new tool will facilitate many additional discoveries in regards to the amazingly diverse optics (Land and Nilsson, 2012) of the world of invertebrate eyes.

Acknowledgements
We thank members of the Buschbeck laboratory for helpful discussions and for feedback on the manuscript, and Winter Partin for assisting us with ophthalmoscope calibrations.

Competing interests
The authors declare no competing or financial interests.

Author contributions
Conceptualization: A.S., E.K.B.; Methodology: A.S., E.K.B.; Validation: A.S.; Formal analysis: A.S., M.O.; Investigation: A.S., M.O., E.K.B.; Resources: E.K.B.; Data curation: E.K.B.; Writing - original draft: A.S., E.K.B.; Writing - review & editing: A.S., M.O., E.K.B.; Visualization: A.S.; Supervision: A.S., E.K.B.; Project administration: A.S., E.K.B.; Funding acquisition: E.K.B.

Funding
This work was supported by the National Science Foundation (grants IOS1050754 and IOS1456757 to E.K.B.).

References
Berry, R. P., Stange, G. and Warrant, E. J. (2007). Form vision in the insect dorsal ocelli: an anatomical and optical analysis of the dragonfly median ocellus. *Vision Res.* **47**, 1394-1409.
Blest, A. D., Hardie, R. C., McIntyre, P. and Williams, D. S. (1981). The spectral sensitivities of identified receptors and the function of retinal tiering in the principal eyes of a jumping spider. *J. Comp. Physiol.* **145**, 227-239.
Cook, T. and Desplan, C. (2001). Photoreceptor subtype specification: from flies to humans. *Semin. Cell. Dev. Biol.* **12**, 509-518.
Cook, T., Zelhof, A., Mishra, M. and Nie, J. (2011). 800 facets of retinal degeneration. *Prog. Mol. Biol. Transl.* **100**, 331-368.
Cronin, T. W. and Goldsmith, T. H. (1981). Fluorescence of crayfish metarhodopsin studied in single rhabdoms. *Biophys. J.* **35**, 653-664.
Eckert, M. (1968). Hell-Dunkel-adaption in aconen Appositionsaugen der Insekten. *Zool. Jb. Physiol. Bd.* **74**, 102-120.
Flitcroft, D. I. (2013). Is myopia a failure of homeostasis? *Exp. Eye Res.* **114**, 16-24.
Franceschini, N. (1972). Pupil and pseudopupil in the compound eye of *Drosophila*. In *Information Processing in the Visual Systems of Anthropods: Symposium Held at the Department of Zoology, University of Zurich, March 6–9, 1972* (ed. R. Wehner), pp. 75-82. Berlin, Heidelberg: Springer Berlin Heidelberg.
Franceschini, N. (1975). Sampling of the visual environment by the compound eye of the fly: fundamentals and applications. In *Photoreceptor Optics* (ed. A. W. Snyder and R. Menzel), pp. 98-125. Berlin, Heidelberg, New York: Springer.
Franceschini, N. (1977). In vivo fluorescence of the rhabdomeres in an insect eye. *Proc. Int. Union Physiol. Sci. XIII* 237, XXVIIth Int. Congr., Paris.
Franceschini, N. (1983). In vivo microspectrofluorimetry of visual pigments. *Symp. Soc. Exp. Biol.* **36**, 53-85.
Franceschini, N. and Kirschfeld, K. (1971). Optical study *in-vivo* of photoreceptor elements in compound eye of *Drosophila*. *Kybernetik* **8**, 1-8.
Franceschini, N., Kirschfeld, K. and Minke, B. (1981). Fluorescence of photoreceptor cells observed in vivo. *Science* **213**, 1264-1267.
Freund, C., Horsford, D. J. and McInnes, R. R. (1996). Transcription factor genes and the developing eye: a genetic perspective. *Hum. Mol. Genet.* **5**, 1471-1488.
Homann, H. (1924). Zum Problem der Ocellenfunktion bei den Insekten. *Z. Vergl. Physiol.* **1**, 541-578.
Horridge, G. A. and Giddings, C. (1971). Movement on dark-light adaptation in beetle eyes of the neuropteran type. *Proc. R. Soc. Lond. B* **179**, 73-85.
Hung, L.-F., Crawford, M. L. J. and Smith, E. L. (1995). Spectacle lenses alter eye growth and the refractive status of young monkeys. *Nat. Med.* **1**, 761-765.
Juse, A., Stūsek, P. and Hamdorf, K. (1989). The properties of photoreconvertible fluorophore systems in insect eyes resemble those of quinones. *J. Comp. Physiol. A* **165**, 789-800.
Kirschfeld, K. and Franceschini, N. (1968). Optische Eigenschaften der ommatidien im komplexauge von *Musca*. *Biol. Cybern.* **5**, 47-52.
Kroger, R. H. H. and Wagner, H.-J. (1996). The eye of the blue acara (*Aequidens pulcher*, Cichlidae) grows to compensate for defocus due to chromatic aberration. *J. Comp. Physiol. A* **179**, 837-842.

Kruizinga, B. and Stavenga, D. G. (1990). Fluorescence spectra of Blowfly metaxanthopsins. *Photochem. Photobiol.* **51**, 197-201.
Land, M. F. (1984). The resolving power of diurnal superposition eyes measured with an ophthalmoscope. *J. Comp. Physiol. A* **154**, 515-533.
Land, M. F. (1969a). Movements of the retinae of jumping spiders in response to visual stimuli. *J. Exp. Biol.* **51**, 471-493.
Land, M. F. (1969b). Structure of the retinae of the principal eyes of jumping spiders (Salticidae: Dendryphanatidae) in relation to visual optics. *J. Exp. Biol.* **51**, 443-470.
Land, M. F. (1990). Direct observation of receptors and images in simple and compound eyes. *Vision Res.* **30**, 1721-1734.
Land, M. F. and Barth, F. G. (1992). The quality of vision int the ctenid spider *Cupiennius salei*. *J. Exp. Biol.* **164**, 227-242.
Land, M. F. and Nilsson, D.-E. (2012). *Animal Eyes*, 2nd edn. Oxford: Oxford University Press.
McBrien, N. A. and Barnes, D. A. (1984). A review and evaluation of theories of refractive error development. *Ophthal. Physl. Opt.* **4**, 201-213.
McFadden, S. A., Howlett, M. H. C. and Mertz, J. R. (2004). Retinoic acid signals the direction of ocular elongation in the guinea pig eye. *Vision Res.* **44**, 643-653.
Menzi, U. (1987). Visual adaptation in nocturnal and diurnal ants. *J. Comp. Physiol. A* **160**, 11-21.
Mizutani, A. and Toh, Y. (1995). Optical and physiological properties of the larval visual system of the Tiger Beetle, *Cicindela chinensis*. *J. Comp. Physiol. A* **177**, 591-599.
Nagata, T., Koyanagi, M., Tsukamoto, H., Saeki, S., Isono, K., Shichida, Y., Tokunaga, F., Kinoshita, M., Arikawa, K. and Terakita, A. (2012). Depth perception from image defocus in a jumping spider. *Science* **335**, 469-471.
Nilsson, D.-E., Hamdorf, K. and Hoglund, G. (1992). Localization of the pupil trigger in insect superposition eyes. *J. Comp. Physiol. A* **170**, 217-226.
Nordstrom, P. and Warrant, E. J. (2000). Temperature-induced pupil movements in insect superposition eyes. *J. Exp. Biol.* **203**, 685-692.
O'Shea, M. and Adams, M. E. (1981). Pentapeptide (proctolin) associated with an identified neuron. *Science* **213**, 567-569.
Pichaud, F. and Desplan, C. (2001). A new visualization approach for identifying mutations that affect differentiation and organization of the *Drosophila* ommatidia. *Development* **128**, 815-826.
Sanes, J. R. and Zipursky, S. L. (2010). Design principles of insect and vertebrate visual systems. *Neuron* **66**, 15-36.
Schaeffel, F., Glasser, A. and Howland, H. C. (1988). Accomodation, refractive error and eye growth in chickens. *Vision Res.* **28**, 639.
Sivak, J. G. (2008). The role of the lens in refractive development of the eye: animal models of ametropia. *Exp. Eye Res.* **87**, 3-8.
Stark, W. S., Ivanyshyn, A. M. and Greenberg, R. M. (1977). Sensitivity and photopigments of R1-6, a two-peaked photoreceptor, in *Drosophila*, *Calliphora* and *Musca*. *J. Comp. Physiol.* **121**, 289-305.
Stavenga, D. G. (1983). Fluorescence of blowfly metarhodopsin. *Biophys. Struct. Mech.* **9**, 309-317.
Stavenga, D. G. (2002). Reflections on colourful ommatidia of butterfly eyes. *J. Exp. Biol.* **205**, 1077-1085.
Stowasser, A. and Buschbeck, E. K. (2014). Multitasking in an eye: the unusual organization of the *Thermonectus marmoratus* principal larval eyes allows for far and near vision and might aid in depth perception. *J. Exp. Biol.* **217**, 2509-2516.
Stowasser, A., Rapaport, A., Layne, J. E., Morgan, R. C. and Buschbeck, E. K. (2010). Biological bifocal lenses with image separation. *Curr. Biol.* **20**, 1482-1486.
Taylor, G. J., Ribi, W., Bech, M., Bodey, A. J., Rau, C., Steuwer, A., Warrant, E. J. and Baird, E. (2016). The dual function of orchid bee ocelli as revealed by X-ray microtomography. *Curr. Biol.* **26**, 1319-1324.
Turnbull, P. R. K., Backhouse, S. and Phillips, J. R. (2015). Visually guided eye growth in the squid. *Curr. Biol.* **25**, R791-R792.
Wallman, J. and Winawer, J. (2004). Homeostasis of eye growth and the question of myopia. *Neuron* **43**, 447-468.
Warrant, E., Bartsch, K. and Gunther, C. (1999). Physiological optics in the hummingbird hawkmoth: a compound eye without ommatidia. *J. Exp. Biol.* **202**, 497-511.
Williams, D. S. and McIntyre, P. (1980). The principal eyes of a jumping spider have a telephoto component. *Nature* **288**, 578-580.